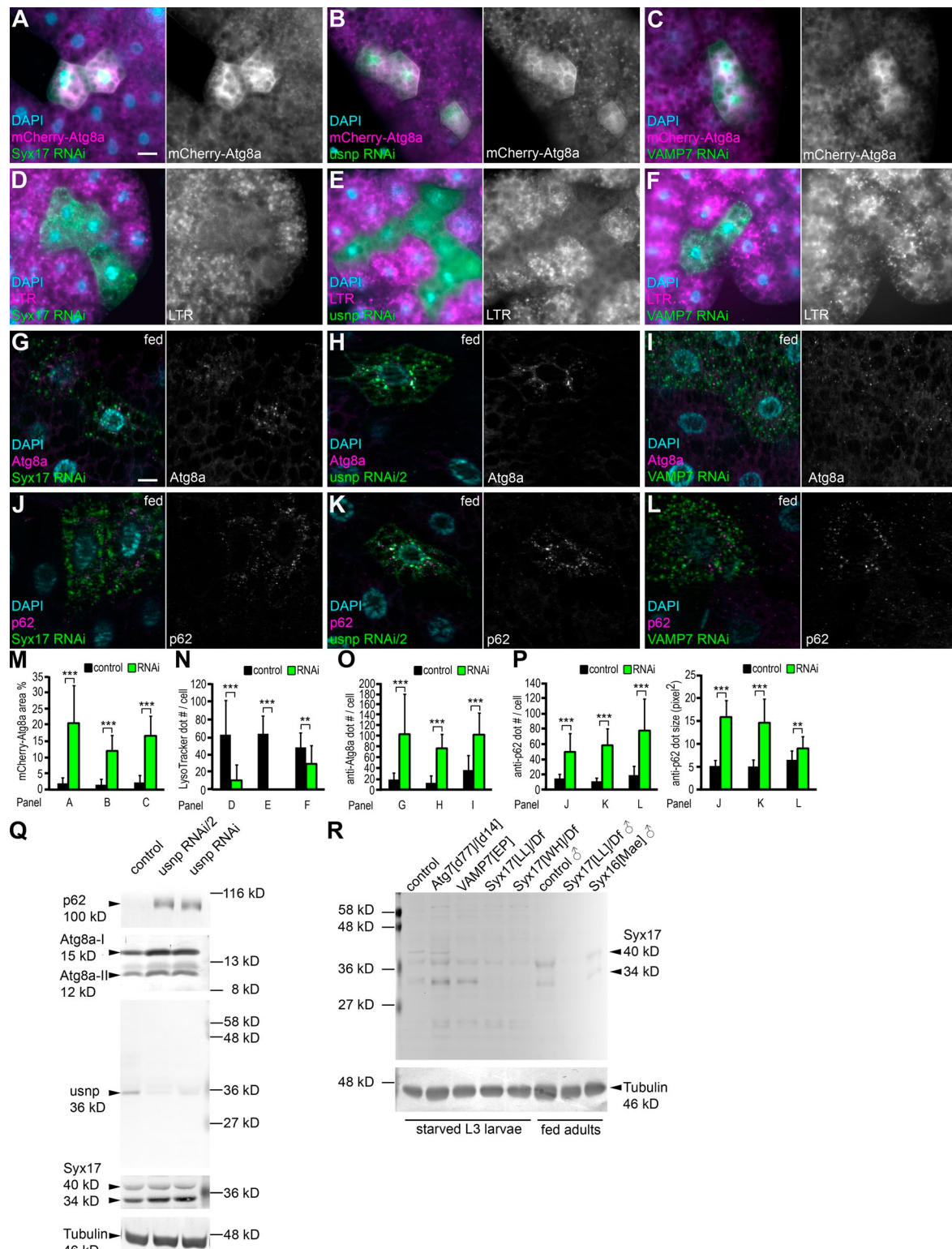
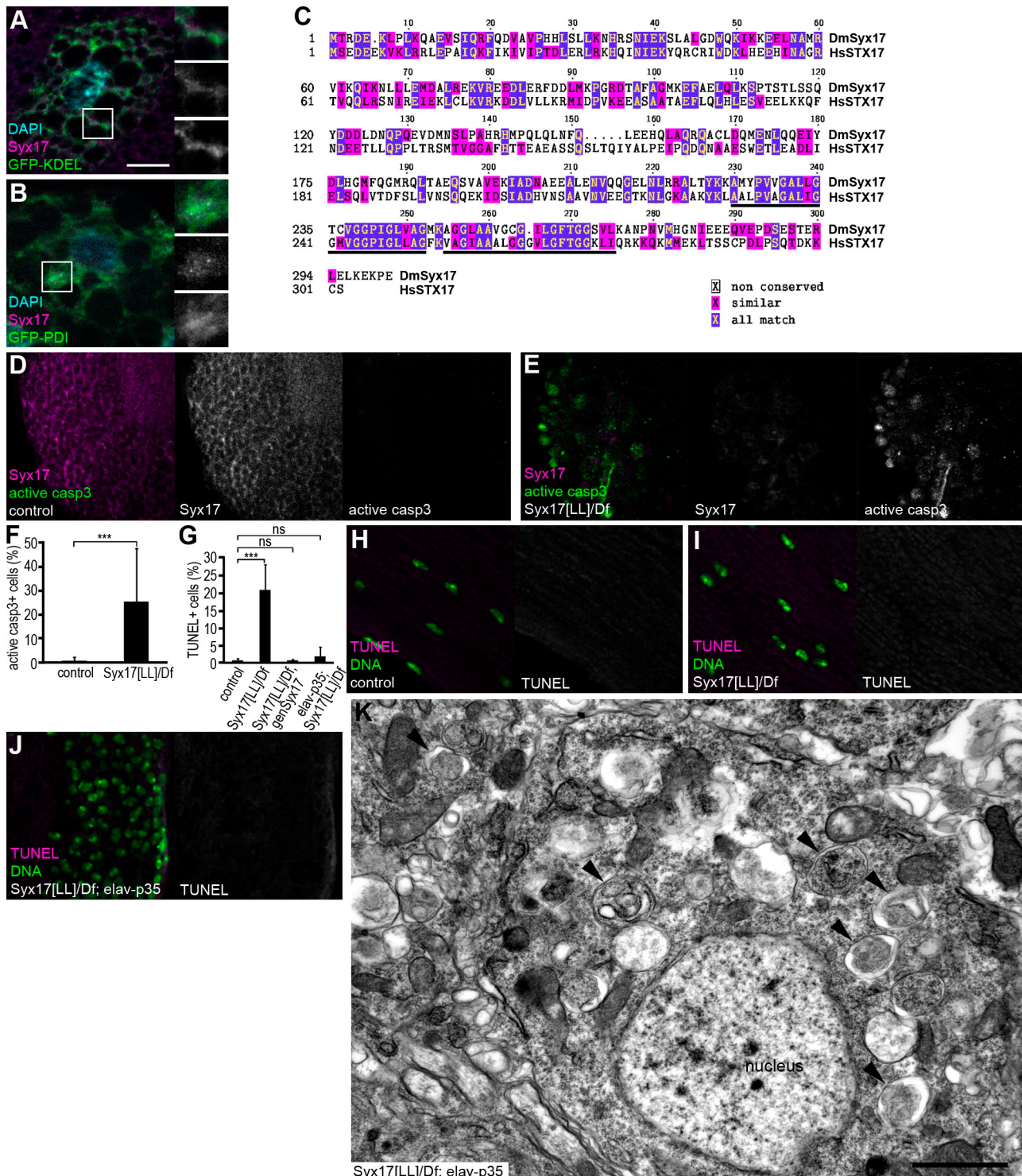


Takáts et al., <http://www.jcb.org/cgi/content/full/jcb.201211160/DC1>

**Figure S1. *Syx17*, *usnp*, and *VAMP7* are required for developmental and basal autophagy.** (A–C) Knockdown of *Syx17* (A), *usnp* (B), or *VAMP7* (C) in GFP-marked fat body cells results in large-scale accumulation of small mCherry-Atg8a dots in wandering L3 stage larvae. (D–F) *Syx17* (D), *usnp* (E), or *VAMP7* (F) RNAi blocks LysoTracker dot formation in wandering animals. (G–I) Atg8a-positive autophagosomes accumulate in *Syx17* (G), *usnp* (H), and *VAMP7* (I) RNAi cells marked by LAMP1-GFP compared with adjacent control fat body cells in well-fed larvae. (J–L) Accumulation of p62 aggregates is obvious in *Syx17* (J), *usnp* (K), and *VAMP7* (L)-depleted fat cells in well-fed larvae. (M–P) Quantification of data shown in A–C (M), D–F (N), G–I (O), and J–L (P).  $n = 10$  for all genotypes. Error bars mark SDs. \*\*,  $P < 0.01$ ; \*\*\*,  $P < 0.001$ . (Q) Systemic RNAi silencing of *usnp* mediated by *Actin-Gal4* results in accumulation of p62 and Atg8a-II in Western blots of L3 stage larval lysates. Anti-*usnp* blot reveals that *usnp* levels are strongly decreased in *usnp* RNAi animals, whereas *Syx17* expression is largely unaffected. (R) Western blot analysis of larval and adult samples shows the specificity of guinea pig anti-*Syx17* antisera. Bars: (A for A–F) 40  $\mu$ m; (G for G–L) 20  $\mu$ m.



**Figure S2. Additional Syx17 data.** (A and B) Endogenous Syx17 localizes to the region of the ER, marked by GFP-KDEL (A) and GFP-protein disulphide isomerase (B). Insets show merged images (top), Syx17 channels (middle), and relevant green channels (bottom) enlarged from boxed areas in A and B. (C) CLUSTALW alignment of *Drosophila* Syx17 and human STX17. Predicted conserved transmembrane domains are underlined. (D and E) No cleaved caspase 3 labeling is detected in brains of control flies (D). Numerous cells are marked by active caspase 3 immunoreactivity, whereas no specific anti-Syx17 staining is detected in Syx17 mutant brains (E). (F and G) Quantification of data shown in D and E (F) and J (this figure) and Fig. 5 (I–K) (G).  $n = 8$  for all genotypes summarized in panels F and G. Error bars mark SDs. \*\*\*,  $P < 0.001$ . (H and I) TUNEL labeling is almost never seen in adult flight muscles of 2-d-old control animals (H; 2/342 muscle cell nuclei were positive) or in muscles of Syx17 mutant animals (I; 4/611 nuclei were positive).  $n = 3$  for both genotypes. (J) TUNEL staining is suppressed by neuron-specific expression of p35 in 2-d-old Syx17 mutant adult brains. (K) Autophagosomes (marked by arrowheads) accumulate in brains of 2-d-old Syx17 mutant adults that express the caspase inhibitor p35 in neurons. Bars: (A for A, B, D, E, and H–J) 20  $\mu$ m; (K) 1  $\mu$ m.

Table S1. List of *Drosophila* homologues of human and yeast SNARE proteins, RNAi and mutant lines for these genes used in this study, and the results of our small-scale RNAi screen

Human	Yeast	Drosophila	CG number	Strains used	Referred to as	Source	mCherry-Atg8a RNAi phenotype
Syntaxin1	Sso1p/Sso2p	Syntaxin1A	CG31136	JF01829 33112		BDSC/TRiP VDRC	No effect No effect
Syntaxin2							
Syntaxin3							
Syntaxin4		Syntaxin4	CG2715	102466		VDRC	No effect
Syntaxin5	Sed5p	Syntaxin5	CG4214	108928		VDRC	Enhancement
Syntaxin6	Tlg1p	Syntaxin6	CG7736	104795		VDRC	No effect
Syntaxin7	Pep12p	Avalanche/ Syntaxin7	CG5081	107264		VDRC	Suppression
Syntaxin8	Syn8p	Syntaxin8	CG4109	JF02436 107014		BDSC/TRiP VDRC	Suppression No effect
Syntaxin10							
Syntaxin11							
Syntaxin12		Syntaxin13	CG11278	102432		VDRC	No effect
Syntaxin16	Tlg2p	Syntaxin16	CG1467	109504 JF01924		VDRC BDSC/TRiP BDSC	No effect No effect
				P{Mae-UAS.6.11}G1176	Syx16[Mae]		
Syntaxin17		Syntaxin17	CG7452	JF01937 PBac{WH}S yx17[f03584] PBac{SAstop DsRed}L06330 Df(3L)Exel8098	Syx17 RNAi Syx17[WH] Syx17[LL]	BDSC/TRiP Harvard Collection DGRC	Small perinuclear dots
Syntaxin18	Ufe1p	Syntaxin18	CG13626	105113		BDSC	
SNAP-23	Sec9p	SNAP-25	CG40452	JF02615		VDRC	Enhancement
SNAP-25	Spo20p	SNAP-24	CG9474	108209		BDSC/TRiP	No effect
SNAP-29		ubisnap	CG11173	JF01883 11173R-2	usnp RNAi usnp RNAi/2	VDRC	No effect
VAMP1	Snc1p/Snc2p	n-synaptobrevin	CG17248	JF03417		BDSC/TRiP	Small perinuclear dots
VAMP2		Synaptobrevin	CG12210	102922		VDRC	Small perinuclear dots
VAMP3							
VAMP4							
VAMP5							
VAMP7		VAMP7	CG1599	1599R-1 P{EP}CG1 599[G7738] Df(2R)BSC132	VAMP7 RNAi VAMP7[EP] VAMP7 Df	NIG-Fly BDSC	Small perinuclear dots
VAMP8							
Ykt6	Ykt6p	Ykt6	CG1515	105648		VDRC	
Sec22a							Enhancement
Sec22b	Sec22p	Sec22a	CG7359	100766		VDRC	No effect
Sec22c							
Bet1	Bet1p	Bet1	CG14084	8420		VDRC	
GS15	Sfl1p						Suppression
GS27	Bos1p	membrin	CG4780	109404		VDRC	No effect
GS28	Gos1p	Gos28	CG7700	100289		VDRC	No effect
Vti1a	Vti1p	Vti1	CG3279	45725 109819		VDRC	No effect
Vti1b			CG44009			VDRC	No effect
Slt1	Slt1p/Use1p	Use1	CG14181	100019		VDRC	No effect
Sec20	Sec20p	Sec20	CG2023	100264		VDRC	No effect

VDRC, Vienna Drosophila RNAi Center; BDSC, Bloomington Drosophila Stock Center; TRiP, Transgenic RNAi Project; DGRC, Drosophila Genetic Resource Center; NIG-Fly, National Institutes of Genetics fly stocks.